J Appl Electrochem (2008) 38:939–945
DOI 10.1007/s10800-008-9500-z

ORIGINAL PAPER

Influence of electrode thickness on the performance of composite electrodes for SOFC

Antonio Barbucci · Mariapaola Carpanese · Andrea P. Reverberi · Giacomo Cerisola · Mireia Blanes · Pere Luis Cabot · Massimo Viviani · Antonio Bertei · Cristiano Nicolella

Received: 12 September 2007 / Revised: 11 January 2008 / Accepted: 24 January 2008 / Published online: 6 February 2008

Abstract Measurements on half-cells consisting of yttria-stabilized zirconia (YSZ) electrolyte pellets and slurry-coated cathodes of different thickness were performed in order to determine the active area for oxygen reduction in composite cathodes of lanthanum strontium manganite (LSM) and YSZ. Electrochemical impedance spectroscopy was used to evaluate the main electrochemical parameters of the cathodic process. The temperature range was between 500 and 900 °C. The experimental results show a remarkable effect of the electrode thickness on the overall reaction rate in all the temperature range. At 750 °C a change in the controlling regime of the oxygen reduction is detectable and has been ascribed to the transition of the rate-determining step from a charge transfer to a mass transfer of the ionic species. A simplified theoretical model of the cathode that accounts for charge transfer and ionic conduction was developed to give insight into the experimental results. The model simulations compared satisfactorily with the experimental data confirming that the behaviour experimentally observed could be approached with the proposed model.

Keywords Active sites · LSM/YSZ composite electrode · Modelling · Electrochemical measurements · Solid oxide fuel cells.

A. Barbucci (✉) · M. Carpanese · A. P. Reverberi · G. Cerisola
Dipartimento di Ingegneria Chimica e Processo, Università di Genova, P.le J.F. Kennedy, 16129 Genova, Italy
e-mail: barbucci@unige.it

A. Barbucci · M. Carpanese · A. P. Reverberi · G. Cerisola · M. Viviani
Consorzio Interuniversitario Nazionale per la Scienza e Tecnologia dei Materiali, Via Giusti, 9, Firenze 50121, Italy

M. Blanes · P. L. Cabot
Departament de Química Física, Facultat de Química, Universitat de Barcelona, Martí i Franquès, 1, Barcelona 08028, Spain

M. Viviani
Istituto per l'Energetica e le Interfasi, CNR, Via De Marini, 6, Genova 16149, Italy

A. Bertei · C. Nicolella
Dipartimento di Ingegneria Chimica, Università di Pisa, V. Diotisalvi 2, Pisa 56126, Italy

1 Introduction

Nowadays the broad commercialization of Solid Oxide Fuel Cell (SOFC) systems is mainly limited by insufficient durability, excessive cost of materials and fabrication processes [1, 2]. As a consequence, current research in SOFC concentrates on the development of highly efficient processes and low cost multi-functional materials for reducing fuel cell stacks and systems cost, improving specific performance and durability [3–6].

One effective approach to cost reduction is lowering the operating temperature without incurring performance losses. Operating cells at 600–700 °C would allow use of less expensive materials for the fabrication of many components, including metallic interconnects, heat exchangers and other structural parts. In addition, a durability improvement is expected because of the less severe operating conditions. On the other hand, ionic conductivity and electrocatalytic activity reduction must be balanced with more efficient ceramic materials [2].

No single material is known to fulfil all the requirements for a given individual cell component. Therefore materials engineering solutions and the development of new fabrication techniques are expected to play a key role in the future.

One of the main points for improving SOFC performance is to understand the extension of the active sites which contribute to oxygen reduction or fuel oxidation at the electrodes. Recently, to understand the performance of SOFC electrodes, the influence of electrode geometry on cell behaviour using circular microelectrodes or patterned electrodes made of dense lanthanum strontium manganite (LSM) has been investigated [7, 8]. It has also been shown that localising the regions where the electrode reactions take place is of great interest, because this can help in electrode design to maximize reaction rate [9, 10].

These approaches are useful because of the opportunity to determine actual local parameters (e.g. three-phase boundary (TPB) length and charge transfer resistivity) and to estimate the role and the sensitivity of micro-structural features (such as particle size, porosity, tortuosity, ionic and electronic conductivity), on the reaction rate. Furthermore, they allow interesting and additional information regarding the role of the many phenomena to be obtained, for instance rate control by adsorption, mass transfer, charge transfer, etc. [11].

In this paper the cathode side of the SOFC receive attention because in hydrogen SOFC this component contributes significantly to the overall losses. Moreover, studies on the cathode side of the cell still constitute a challenge because the oxygen reduction process is not completely understood.

The aim of the experimental approach and the theoretical analysis presented is to contribute to the understanding of the distribution of active sites for oxygen reduction on composite cathodes of different thickness. Accordingly, the electrode thickness of these cathodes, adopting the half-cell configuration of the SOFC, has been modulated over a wide range, measuring their electrochemical activity in air by means of potentiodynamic polarization and electrochemical impedance spectroscopy (EIS). We have chosen the common materials employed in SOFC, so that no mixed ionic-electronic conduction occurs in single phases and, in addition, charge transfer processes are mainly localized at the TPBs.

2 Experimental

Typical three-electrode test cells were used to perform electrochemical investigations on composite cathodes in air. The details of the experimental set up and techniques to study the half-cell characteristics of the cathodes have been reported previously [12] and only the essential features are given here. The electrolyte pellet was made by pressing 2.5 g of 8 mol% Y_2O_3 + 92 mol% ZrO_2 powders (TZ-8YS Tosoh powder with 0.3 μm particles assembled in 40 μm agglomerates) at 12 tons and sintering at 1,500 °C for 5 h. The final result was a ceramic disk 20 mm in diameter and about 2-mm thick. This thickness was chosen to avoid measurement errors due to the misalignment of the working and counter electrodes [13]. The working electrodes (cathodes) were prepared by overnight wet ball-milling of equal volumes of YSZ and $(La_{1-x}Sr_x)_y MnO_{3 \pm \delta}$ ($x = 0.25$ and $y = 0.95$. Praxair, about 0.3 μm). Then the mixture was dried and diluted in α-Terpineol (Aldrich). Further milling was performed to obtain a paste that could easily be applied to the YSZ pellet surface by slurry coating. The electrode was then sintered at 1,100 °C for 1 h. From a geometrical point of view, the LSM/YSZ electrodes were arranged on the circular surfaces of the solid electrolyte in order to achieve experimental conditions based on cylindrical symmetry. LSM/YSZ cathodes were prepared at different thickness ranging between 5 and 100 μm using different masks. In order to reach equi-potential conditions (i.e. homogeneous distribution of current lines) a thin layer of current collector, made up of coarse particle size, highly conductive paste prepared by mixing the coarse LSM with terpineol, was applied to the working electrode surface in contact with the external circuit wires. A Pt reference (Pt ink 6926 Engelhard, particle dimension around 12 μm) electrode was painted around the working electrode, and care was taken to leave as large a distance as possible between the reference and working electrodes in order to prevent systematic errors in the measurements of the electrochemical characteristics. A Pt counter-electrode, having the same shape and position as the working electrode, was painted on the opposite side of the electrolyte pellet. The reference and counter electrodes were fixed to the pellet using a sintering treatment at 900 °C for about 1 h.

The morphologic observation of the cell was carried out after the electrochemical experiments to control the uniformity of the electrode thickness. The cells were embedded in epoxy resin, cut by a diamond disk and then observed by scanning electron microscopy (SEM). The electrode thickness was measured over the whole section. Homogeneous electrodes with deviations from the nominal values not higher than ± 1 μm were obtained for thin electrodes (5-, 10-μm thick) and deviations about ±2–3 μm for thicker ones (>20-μm thick).

The cells were place in a rig in an alumina shoe that slid over an alumina supporting tube [14] inserted in a tubular furnace. Measurements were carried out between 500 and 900 °C. The temperature was controlled by a thermocouple placed close to the cell (1 cm).

The wires used to connect the cell to the electrochemical instruments were platinum. The cell and the wires were shielded to reduce noise. The electrochemical investigations consisted of impedance analysis (EIS) and potentiodynamic measurements. The EIS analyses were performed using a 1286 Solartron electrochemical interface

and a 1260 Solartron Frequency Response Analyzer over a frequency range of 0.1 Hz–100 kHz with 20 mV A.C. signal amplitude, at equilibrium potential and under polarization. Potentiodynamic measurements were performed using the same instrumentation. The cell was left at the highest temperature for 24 h before starting the measurements.

3 Results and discussion

Typical impedance plots for electrodes of different thickness at 700 °C are depicted in Fig. 1. The polarization resistance (R_p) was obtained as the difference of the intercepts of the frequency dispersion curves at low and high frequencies in the Nyquist plot.

The R_p values obtained from the Nyquist diagrams for the different half-cells and temperatures are plotted in Fig. 2a, b. The polarization resistance generally decreases as the electrode thickness increases up to about 40 µm, with a further slight increase for greater thickness. A general decrease of R_p with increasing thickness has been reported by other authors in different conditions [15, 16]. For each series at constant temperature a decrease in the polarization resistance up to about 50% from the value of the thinnest electrode is reached at about 40 µm. The R_p values always increased slightly for thicker electrodes. However, the experimental error did not allow extrapolation to very high thickness to obtain limiting values. On the other hand, measurements for thickness higher than about 80 µm are interesting from a practical point of view.

Impedance measurements performed at increasing negative overpotentials, η, display a regular decrease of the semicircle size of the frequency dispersion curves. Figure 3 shows this behaviour for half-cells with 10-µm thick cathode at different overpotentials and 700 °C. The trend of the polarization resistance as a function of the applied cathode

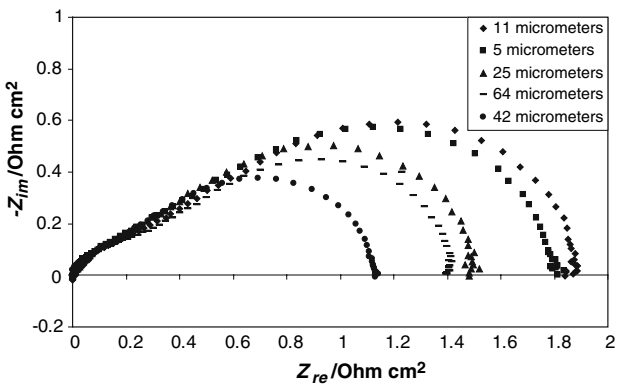

Fig. 1 Nyquist plots of some half-cell with different thick cathodes obtained in air at open circuit voltage and 700 °C

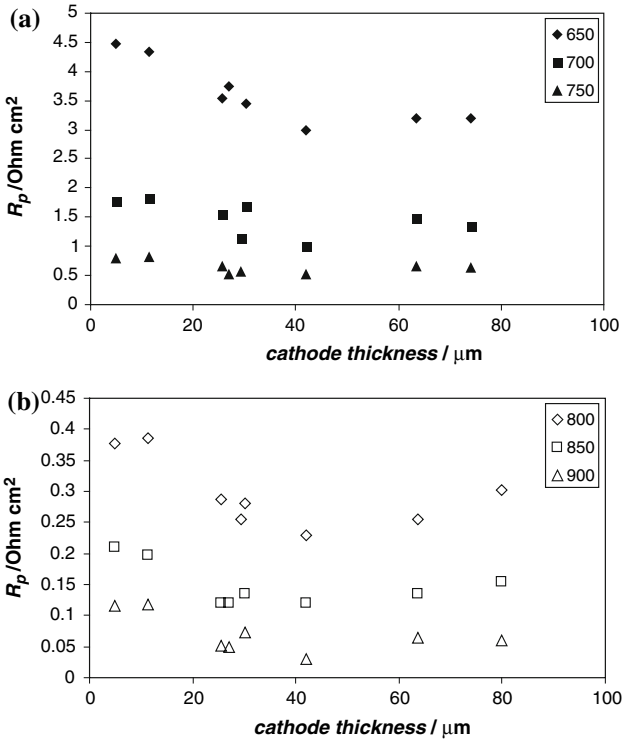

Fig. 2 Values of R_p as a function of the electrodes thickness, at different temperatures. Operating conditions: air, open circuit voltage

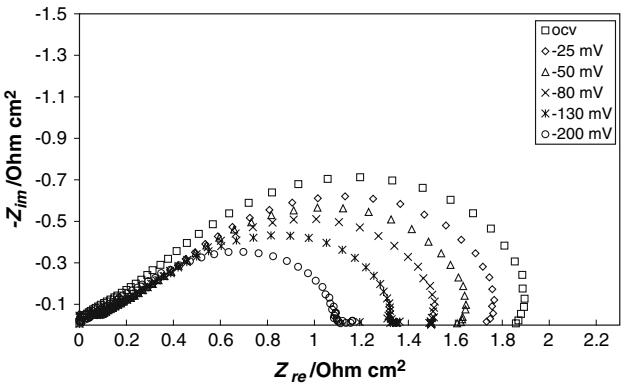

Fig. 3 Nyquist plots of the cell with the 10-micron thick cathode, at different cathodic overpotentials. Operating conditions: 700 °C, air

overpotential is presented in Fig. 4 for two types of cathode (10- and 80-µm thick) at 700, 750 and 800 °C. The diagrams highlight a good linear trend of the data for 700 and 750 °C. At 750 °C the correlation factor (R^2) is remarkably lower than unity but a linear relationship between the logarithm of the inverse of R_p and the overpotential is still valid. At 800 °C the linear dependence is completely lost. Such a linear relation can be explained by an activation control regime of the oxygen reduction as predicted by the Butler-Volmer equation neglecting the anodic contribution when high cathodic overpotentials are applied.

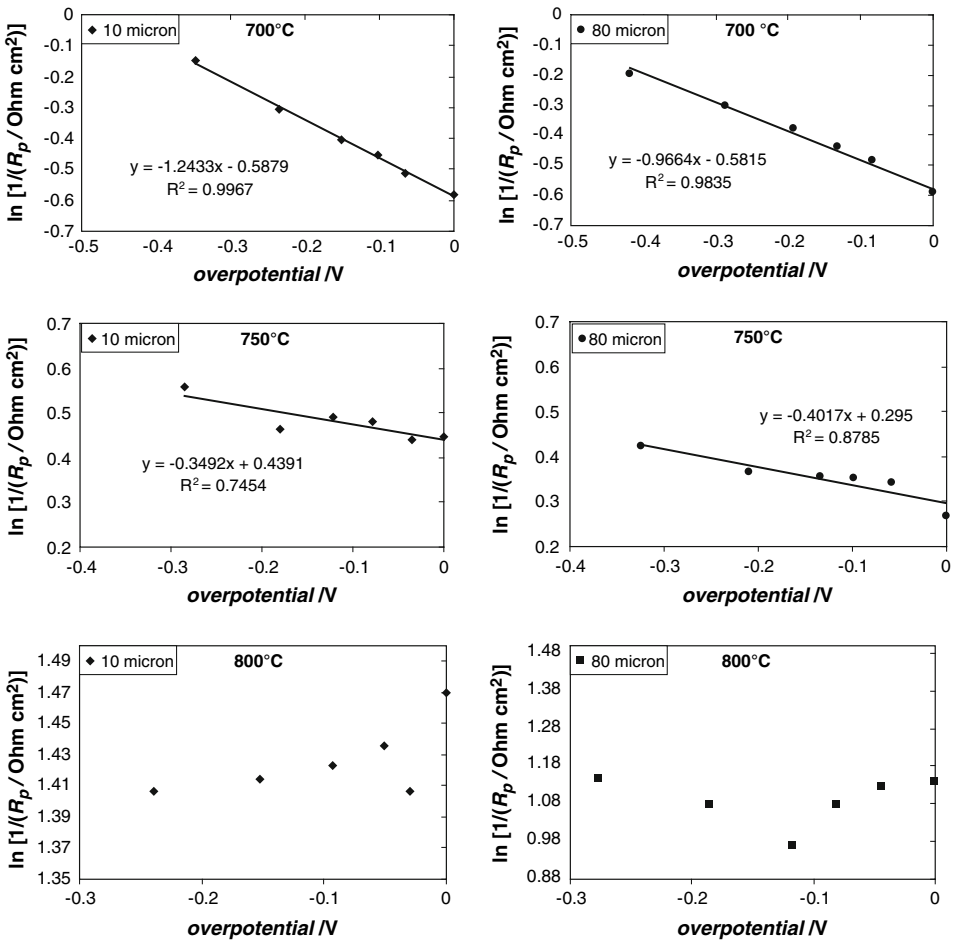

Fig. 4 Trends of $\ln(1/R_p)$ vs. over potential. Data extracted from impedance plots at different biases (as shown in Fig. 3). Left: cell with a 10-µmm thick cathode; right: cell with a 80-µm thick cathode

The results given in Fig. 4 then suggest that at about 750–800 °C a transition in the overall reaction from charge transfer control to mass transfer control [12, 17] probably, takes place. Since the gas diffusion coefficient of molecular oxygen is much faster than the diffusivity of oxygen ions in the ionic path of the electrode, it is reasonable to think that the deviation from the linear behaviour between $\ln(1/R_p)$ and η is due to ionic transport within the electrode [10]. The charge transfer resistance and ionic conduction of O^{2-}, both increase exponentially with inverse of temperature $1/T$, but the rate of oxygen ion production at the active sites has a steeper dependence on $1/T$ with respect to ionic conductivity [18] (Fig. 5). Moreover, to consider the ionic conductivity of YSZ within the electrode as a key factor is justified because the sintering temperature of the electrode, and hence of YSZ in this case, is limited to 1,100 °C, due to the stability/reactivity of LSM. The difference in the conductivity of YSZ sintered at 1,100 °C with respect to normal YSZ sintered at 1,500 °C is remarkable [19].

In order to interpret the results, a simplified model based on the fundamental idea that charge transfer and ion transport play the main role in the overall oxygen reaction has been considered. The circuit describing the possible behaviour of the composite cathode considering a discrete approach is shown in Fig. 6a, where I_{tot} refers to the total current passing through the cathode. In the composite cathode the electrons react at active sites distributed into the electrode or at the true interface between the composite electrode and the electrolyte. In the first case, providing that oxygen gas is present in the electrode pores, the electrons are incorporated into the oxygen ions that further continue their motion (J_v) toward the dense electrolyte (Fig. 6a, volume path). The second possibility is that the electrons pass through all the electrode thickness δ to react directly (J_S) at the true interface (Fig. 6a, surface path). For these two parallel paths it is possible to extract the total resistance. In fact, assuming that the electrodic reaction into the electrode volume takes place at half of the thickness, which is a very simplified situation but represents the mean one, the resistance for the volume path is:

$$R_v = \rho_{el}\tau_{el}\frac{\delta}{2} + \frac{R_{cont}}{N_v\delta} + \rho_{io}\tau_{io}\frac{\delta}{2} \quad (1)$$

and, for the surface path:

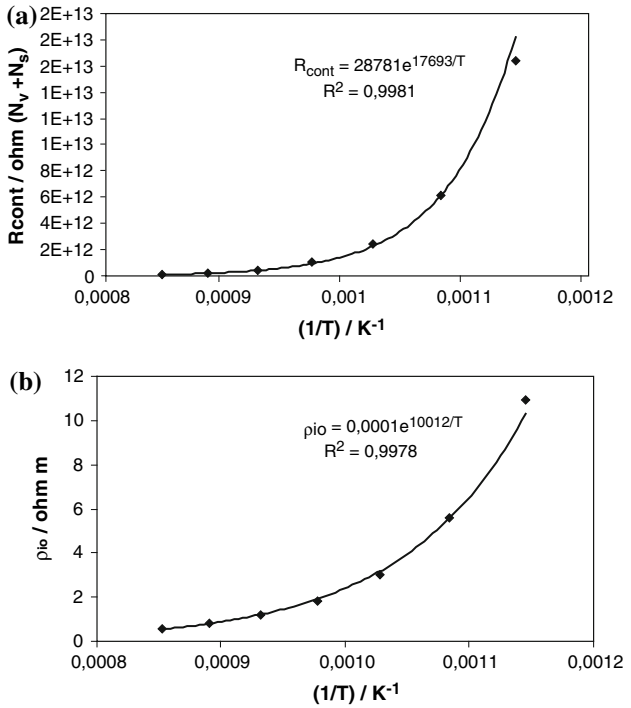

Fig 5 Exponential dependence of charge transfer resistance (determined on electrode of pure LSM applied on YSZ electrolyte [18]) (**a**) and ionic resistance of YSZ (**b**) on $1/T$

$$R_s = \rho_{el}\tau_{el}\delta + \frac{R_{cont}}{N_s} \tag{2}$$

The parameters ρ_{io} and ρ_{el} are the ionic and electronic resistivity (Ωm) of YSZ and LSM respectively. For these parameters the data reported in Table 1 were used. While ρ_{io} is strongly dependent on T, ρ_{el} has been considered constant due to the very small variation in the range of temperature considered ($\rho_{el} = 2.02 \times 10^{-3}$ Ωm [20, 21]). The parameters τ_{io} and τ_{el} are related to the tortuosity of the electronic and ionic paths, respectively; they are necessary for the correct estimation of the ohmic loss in the conductors. R_{cont} is the charge transfer resistance defined as:

$$R_{cont} = \frac{RT}{FJ_0} \tag{3}$$

where J_0 is the exchange current related to the number of contacts ($J_0 = j_0\ a_n$, where j_0 is the exchange current related to the active area and a_n is the specific contact area per number of contacts). The kinetic parameter J_0 is determined at any temperature by fitting the impedance data collected on a cell with a cathode made of pure LSM. The parameter N_v (m^{-3}) is related to the number of useful contacts (TPB) into the electrode feed by electrons and connected with the dense electrolyte by an ionic path; N_s (m^{-2}) represents the same useful contact but only those which are concentrated at the true interface electronically

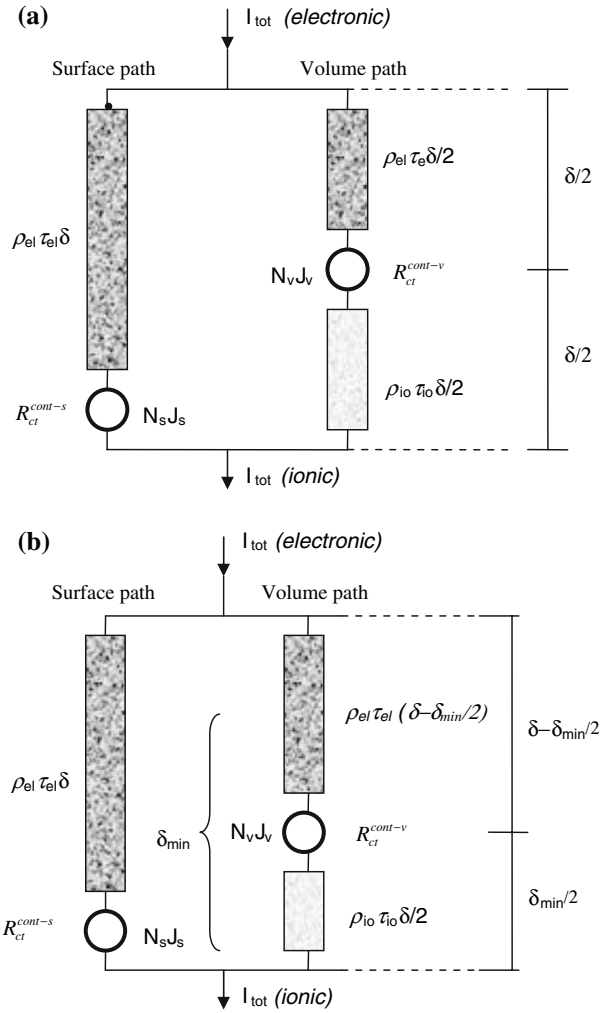

Fig. 6 Simplified circuit model for the interpretation of the impedance results

Table 1 Values of the ionic resistivity of YSZ and LSM

T (°C)	ρ_{io} (Ωm)
500	64.80
600	10.92
700	2.99
800	1.19
900	0.58

connected to the current collector. Both these parameters have been calculated by the percolation theory using the relations developed by Bouvard and Lange [22].

In this simplified model it should be taken into account that the potential active sites increase with the electrode thickness. On the other hand, as the electrode reaction of the volume path is assumed at half height ($\delta/2$) the ionic contribution to the resistance in this path is expected to increase monotonically. This leads to the possibility to have an increase of R_v with δ In other words, let us assume that at a given current density with an electrode thickness

equal to δ the electrons react aver all the volume of the electrode. When δ is increased in $\Delta\delta$, the new volume on the top of the electrode produces oxygen ions whose pathway to reach the true electrolyte has a higher resistivity. If this resistivity is so high that at the end the total overpotential to overcome is higher than the overpotential corresponding to the thicker electrode $\delta\Delta\delta$), the new volume would be used only for the passage of electrons, without contributing to oxygen reduction.

In fact, if we increase δ up to infinity, the reaction will not involve all the volume of the electrode, because the ohmic loss of the oxygen ions produces an infinite voltage loss. Then, assuming that they can flow through the electrocatalyst without any resistance, the electrons will move toward the true interface till they find favourable conditions to react, at a distance $\delta_{\min}$, in which the decrease in current density due to the extension of the TPB is not penalized by the ohmic loss of the oxygen ions.

Then, for $\delta > \delta_{\min}$ (Fig. 7b) the value of R_v is calculated as:

$$R_v = \rho_{el}\tau_{el}\left(\delta - \frac{\delta_{\min}}{2}\right) + \frac{R_{cont}}{N_v\delta_{\min}} + \rho_{io}\tau_{io}\frac{\delta_{\min}}{2} \quad (4)$$

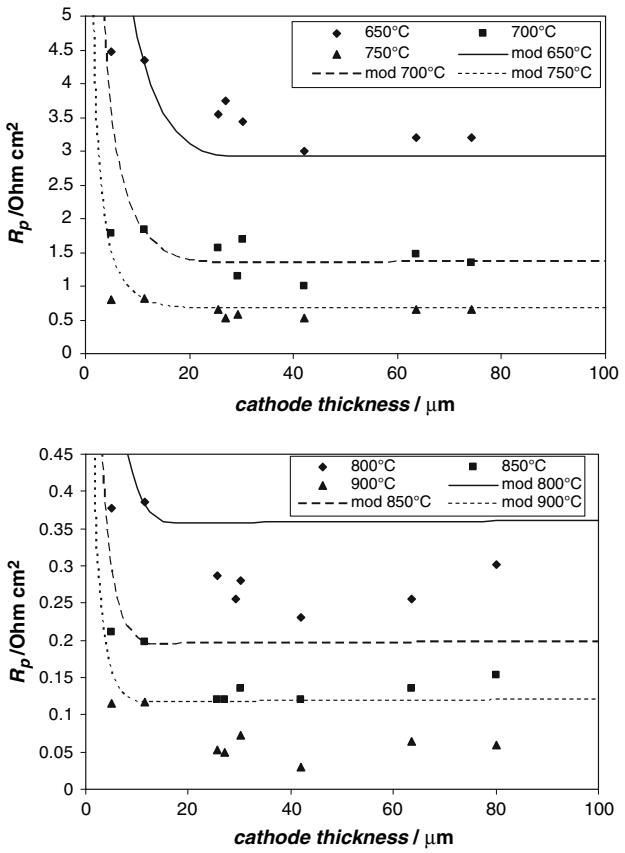

Fig. 7 Comparison of the experimental and simulated results ($N_v = 5.45\times 10^{19}$ m^{-3}, $N_s = 1.62 \times 10^{12}$ m^{-2}, $\tau = 1.82$)

In this last situation an increase in R_v with δ is expected due to the electronic resistivity of the electrocatalyst. However this is a factor of secondary importance due to the low electronic resistivity of LSM compared to the other source of losses.

The total resistance of the process, which should be equal to the polarization resistance, can be calculated as:

$$R_p = \frac{R_s R_v}{R_s + R_v} \quad (5)$$

In Fig. 7 the experimental data presented in Fig. 2 have been compared with those calculated by the model. The model agrees well with the experimental result at 650, 700 and 750 °C. For higher values of T the general trend of the experimental data is followed, but the model looses accuracy. Of course the idea presented here is very basic but it seems that the assumptions made and the general approach give promising results. The advantage of this tool is its simplicity and this could constitute the starting point for a refined version of the model which, with further optimization of the parameters (τ_{el}, τ_{io}, N_v, N_s,...), could lead to better results.

4 Conclusions

The experimental results show a remarkable effect of electrode thickness on the overall reaction rate in the whole temperature range investigated. An optimum electrode thickness of about 40 microns has been highlighted. Regarding the oxygen reduction reaction at 750 °C a change in the controlling regime is detectable and has been ascribed to the transition of the rate determining step from charge transfer to mass transfer of the ionic species. The simple theoretical model proposed for the interpretation of the experimental results confirms this idea and supplies further useful information. However, optimization of the model is necessary, especially regarding the estimation of morphological parameters of the electrode. These basic parameters play a relevant role in the understanding of the electrochemical process and in electrode design.

Acknowledgements The authors gratefully acknowledge financial support of the Italian project "FISR: Nanosistemi Inorganici ed Ibridi per lo Sviluppo e l'Innovazione di Celle a Combustibile".

References

1. Badwal SPS (2001) Solid State Ionics 143:39
2. Steele BCH, Heinzel A (2001) Nature 414:345
3. Singh P, Minh NQ (2004) Int J Appl Cer Technol 1(1):5
4. Yuan J, Sundén B (2005) Trans of the ASME 127:1380
5. Steele BCH (2000) Solid State Ionics 129:95
6. Peña-Martínez J, Marrero-López D, Pérez-Coll D, Ruiz-Morales JC, Núñez P (2007) Electrochim Acta 52:2950

7. Brichzin V, Fleig J, Habermeier H-U, Maier J (2000) Electroch Sol St Lett 3(9):403
8. Radhakrishnan R, Virkar AV, Singhal SC (2005) J Electroch Soc 152:A210
9. Fleig J, Maier J (2004) J Europ Cer Soc 24:1343
10. Schneider LCR, Martin CL, Bultel Y, Dessemond L, Bouvard D (2007) Electrochim Acta 52:3190
11. Adler SB (2004) Chem Rev 104:4791
12. Barbucci A, Carpanese P, Cerisola G, Viviani M (2005) Solid State Ionics 176:1753
13. Winkler J, Hendriksen PV, Bonanos N, Mogensen M (1998) J Electrochem Soc 145(4):1184
14. Macdonald JR (1987) Impedance spectroscopy. John Wiley & Sons, New York, Inc. p 214
15. Dusastre V, Kilner JA (1999) Solid State Ionics 126:163
16. Tanner CW, Fung KZ, Virkar AV (1997) J Electrochemical Soc 144:21
17. Chen XJ, Chan SH, Khor KA (2004) Electrochim Acta 49:1851
18. Carpanese MP (2003) Thesis, University of Genova
19. Barbucci A, Carpanese P, Cerisola G, Viviani M, Nicolella C (2007) Electrochim. Acta submitted
20. Yi JY, Choi GM (2002) Solid State Ionics 148:557
21. Li Y, Kilner JA, Carolan MF (2005) Solid State Ionics 176:937
22. Bouvard D, Lange FF (1991) Acta Metall Mater 39(12):3083